Removal of Chromium (VI) from Water by Clays

ARTICLE *in* INDUSTRIAL & ENGINEERING CHEMISTRY RESEARCH · SEPTEMBER 2006

Impact Factor: 2.59 · DOI: 10.1021/ie060586j

2 AUTHORS, INCLUDING:

Krishna G. Bhattacharyya
Gauhati University
105 PUBLICATIONS **3,870** CITATIONS

SEE PROFILE

Adsorption of Chromium(VI) from Water by Clays

Krishna G. Bhattacharyya*,† and Susmita Sen Gupta‡

Department of Chemistry, Gauhati University, Guwahati 781014, Assam, India, and Department of Chemistry, B N College, Dhubri 783324, Assam, India

Interactions of kaolinite and its modified forms, acid-activated kaolinite, poly(oxozirconium) kaolinite, and tetrabutylammonium kaolinite, have been investigated for their utilization as adsorbents for Cr(VI) in aqueous medium. The variables are Cr(VI) concentration, amount of kaolinite or its modified forms, pH, interaction time, and temperature. The adsorption is strongly dependent on the pH of the medium with Cr(VI) uptake increasing from pH 1.0 to pH 7.0, after which the uptake decreases. The process attains equilibrium within 240 min. The kinetics of the interactions is tested with respect to pseudo-first-order, second-order, Elovich, liquid film diffusion, and intraparticle diffusion models, and it is seen that the interactions do not follow a simple model. The adsorption process, however, gives a good fit with both the Langmuir and Freundlich isotherm equations. The Langmuir monolayer capacity of the clay adsorbents is from 10.6 to 13.9 mg g^{-1}. The adsorption process is endothermic ($\Delta H = 30.4-63.9$ kJ mol^{-1}) accompanied by an increase in entropy ($\Delta S = 88.4-198.1$ J mol^{-1} K^{-1}) and decrease in Gibbs energy. The results have shown that acid-activated kaolinite has the largest adsorption capacity followed by nonactivated kaolinite, ZrO−kaolinite, and TBA−kaolinite.

1. Introduction

Hexavalent chromium, Cr(VI), is toxic to all life forms and is considered a priority pollutant. Cr(VI) finds use in a number of industries, for example, ink manufacturing, dyes, paints, metal plating, automobile spare parts, and petroleum refining.[1] Exposure to Cr(VI) causes irritation and corrosion of skin, respiratory tract, and probably lung carcinoma.[2] Epigastric pain, nausea, vomiting, severe diarrhea, and hemorrhage are other deadly consequences of Cr(VI) contamination. The International Agency for Research on Cancer (IARC) has classified inhaled Cr(VI) as a human carcinogen.[3]

The technologies available for controlling heavy metals in the environment include chemical precipitation, ion exchange, solvent extraction, reverse osmosis, and adsorption.[4] Adsorption has been a very effective and economical method for removal, recovery, and recycling of metals from wastewater.[5] Different conventional and nonconventional adsorbents have been cited in the literature for this purpose such as red mud,[6] coconut coirpith,[7] sewage sludge,[8] silica,[9] tree fern,[10] bone char,[11] polymetallic sea nodule,[12] and modified zeolites.[13] Removal of Cr(VI) has been tried on adsorbents such as activated carbon,[14] *Spirogyra* biosorbent,[15] maple sawdust,[16] fly ash,[17,18] and layered double hydroxide.[19]

The clay minerals in soil play the role of a natural scavenger by filtering out pollutants from water through both ion exchange and adsorption mechanisms. Clays are extremely fine particles exhibiting chemical properties of colloids.[20] The high specific surface area, chemical and mechanical stability, layered structure, high cation exchange capacity (CEC), etc., have made clays excellent adsorbent materials. In the case of kaolinite, the CEC is confined primarily to the surface, in contrast to smectites and illites where a large part of the CEC belongs to interior sites.[21] Therefore, to study purely surface processes, kaolinite may be an ideal material.

Acid treatment of clay minerals is an important control over mineral weathering and genesis.[22,23] Such treatments can often replace exchangeable cations with H^+ ions and release Al^{3+} and other cations out of both tetrahedral and octahedral sites, but leaving the SiO_4 groups largely intact.[24] It was reported that acid activation followed by thermal treatment increases the adsorbent capacity to a good extent.[25]

Intercalation of clays cross-linked with inorganic or organic clusters has received wide attention recently as shape-selective catalysts, separating agents, supports, adsorbents, etc. Clays intercalated with metal oxides are of enormous importance because of their high thermal stability, high surface area, and intrinsic catalytic activity. These materials are usually prepared by ion-exchanging cations in the interlayer region of swelling clays with bulky alkylammonium ions, polynuclear complex ions bearing inorganic ligands (hydroxo ligand, chloro ligand), large metal complex ions bearing organic ligands, etc. The intercalated species are capable of preventing the collapse of the interlayer spaces, propping open the layers as pillars, and forming an interlayer space. On heating, the intercalated inorganic species are converted to metal oxide clusters, generating a stable microporous structure with a high surface area.

Burch and Warburton[26] introduced Zr tetramers from fresh zirconyl chloride solution into montmorillonite. Pereira et al.[27] prepared pillared Zr−montmorillonite in a similar way. Preparation of pillared montmorillonite with TMA (tetramethylammonium), TMP (tetramethylphosphonium), and TMPA (trimethylphenylammonium) cations has also been reported.[28,29] Ohtsuka et al.[30] have shown that the zirconium species exist in a number of polynuclear ionic species in zirconium oxychloride solution and, as a result, three kinds of microporous clays with 7-, 12-, and 14-Å interlayer spacings are produced.

Natural clays and their modified forms have found use in metal ion removal from aqueous solutions. Illite has been used for Cd(II),[31] natural and Na-exchanged bentonites have been used for Cr(III), Ni(II), Zn(II), Cu(II), and Cd(II),[32] sepiolite has been used for Co(II),[33] kaolinite has been used for Mn(II), Co(II), Ni(II), and Cu(II)[34] and also for Cd(II) and Co(II),[35] smectite has been used for Cu(II),[36] modified montmorillonite

* To whom correspondence should be addressed. Fax +91 361 2700311. E-mail: krishna2604@sify.com.
† Gauhati University.
‡ B. N. College.

10.1021/ie060586j CCC: $33.50
Published on Web 09/07/2006

Table 1. Experimental Conditions

type of study	amount of clay (g/L)	Cr(VI) concn (mg/L)	pH	temp (K)	interaction time (min)
effect of pH	2	50	1, 2, 3, 4, 5, 6, 7, 8, 9, 10	303	240
effect of clay amount	2, 3, 4, 5, 6	50	4.6	303	240
effect of initial Cr(VI) concn	2	10, 20, 30, 40, 50	4.6	303	240
kinetics	2	50	4.6	303	20, 40, 60, 90, 120, 150, 180, 240, 300, 360
isotherm	2	10, 20, 30, 40, 50, 75, 100,150, 200, 250	4.6	303	240
thermodynamics	2	10, 20, 30, 40, 50	4.6	303, 308, 313	240

has been used for Cu(II) and Zn(II),[37] 1:10 phenanthroline-grafted Brazilian bentonite has been used for Cu(II),[38] acid-activated kaolinite and montmorillonite have been used for Pb(II),[39] etc.

In the present work, adsorptive removal of Cr(VI) from aqueous solution was studied by using kaolinite and three modified forms, viz., acid-activated kaolinite, poly(oxozirconium) kaolinite (ZrO−kaolinite), and tetrabutylammonium kaolinite (TBA−kaolinite) under various environmental conditions.

2. Experimental Section

2.1. Reagents. Reagent grade chemicals, viz., H_2SO_4 (E. Merck, Mumbai, India), $ZrOCl_2 \cdot 8H_2O$ (Loba Chemie, Mumbai, India), and tetrabutylammonium bromide, $(C_4H_9)_4N^+Br^-$ (CDH, Mumbai, India) were used. A stock solution containing 1000 mg of Cr(VI) per liter was prepared by dissolving $K_2Cr_2O_7$ (E. Merck, Mumbai, India) in double-distilled water and was used to prepare the adsorbate solutions by appropriate dilution. The pH of the aqueous solution of Cr(VI) as prepared was 4.6.

2.2. Clay Adsorbents. Kaolinite used for all experiments was KGa-1b (K1) obtained from the University of Missouri−Columbia, Source Clay Minerals Repository.

Acid-activated kaolinite (K2) was prepared by the procedure of Espantaleon et al.[40] For this, 20 g of kaolinite was refluxed with 200 mL of 0.25 M H_2SO_4 for 3 h. The resulting activated clay was centrifuged and washed with water several times until it was free of SO_4^{2-} and dried at 383 K in an air oven until constant weight was attained.

Poly(oxozirconium) kaolinite (K3) was prepared by the procedure of Burch and Warburton.[26] A suspension was made by mixing 4 g of the clay with 100 mL of double-distilled water followed by slow addition of 100 mL of 0.1 mol dm^{-3} solution of $ZrOCl_2$ under constant stirring. Stirring was continued for 24 h, after which the suspension was filtered and the clay was washed with water until it was free of Cl^- ion. The clay was dried in an air oven at 373 K for 30 min.

The TBA derivative (TBA−kaolinite, K4) was prepared by taking 10.0 g of kaolinite presaturated with Na^+ ions (stirring with 1 L of 1 M NaCl solution for 12 h) and then allowing it to settle.[41] The supernatant liquid was discarded and the process was repeated twice with fresh 1 M NaCl solutions. The clay was separated by centrifugation and washed with water to make it Cl^- free. The Na^+-saturated clay was then mixed with water and 300 mL of aqueous TBA−Br solution in a total volume of 1 L, with TBA−Br content 5 times the CEC of the clay. The mixture was centrifuged and washed with water until it was free of Br^-. The resulting organoclay was dried in an air oven at 373 K for 30 min.

Kaolinite and its modified forms were calcined before they were used as adsorbents (kaolinite, acid-activated kaolinite, and ZrO−kaolinite at 773 K and the TBA derivative at 973 K for 10 h; the higher temperature in case of the TBA derivative was necessary to get rid of the organic template).

2.3. X-ray Diffraction (XRD) Measurement. A Phillips Analytical X-ray spectrometer (PW 1710) using Cu Kα radiation was used for characterizing the adsorbents.

2.4. Surface Area Measurement. The surface areas of the clay adsorbents were estimated following Sears' method.[42] A sample containing 0.5 g of clay was acidified with 0.1 N HCl to pH 3−3.5. The volume was made up to 50 mL with distilled water after addition of 10.0 g of NaCl. The titration was carried out with standard 0.1 M NaOH in a thermostatic bath at 298 ± 0.5 K to pH 4.0, and then to pH 9.0. The volume, *V*, required to raise the pH from 4.0 to 9.0 was noted, and the surface area (*S*) was computed from the following equation:

$$S\ (\mathrm{m^2/g}) = 32V - 25 \qquad (1)$$

2.5. Cation Exchange Capacity. The CEC of the clays was estimated by using the copper bis(ethylenediamine) complex method.[43] The CEC was calculated from the following formula:

$$\mathrm{CEC\ (mequiv/100\ g)} = MSV(x - y)/1000m \qquad (2)$$

where *M* is the molar mass of the complex, *S* is the concentration of the thio solution, *V* is the volume (mL) of the complex taken for iodometric titration, *m* is the mass of adsorbent taken (g), *x* is the volume (mL) of thio required for blank titration (without the adsorbent), and *y* is the volume (mL) of thio required for the titration (with the adsorbent).

2.6. Adsorption Experiments. Batch adsorption experiments were carried out in 100 mL Erlenmeyer flasks by mixing together a constant amount of clay with a constant volume of the aqueous solution of Cr(VI). The contents in the flasks were agitated by placing them in a constant temperature water bath thermostat for a known time interval. The mixture was then centrifuged (Remi R 24), and Cr(VI) remaining unadsorbed in the supernatant liquid was determined with atomic absorption spectroscopy (Varian SpectrAA 220 with air−acetylene oxidizing flame, wavelength 429.1 nm, lamp current 5 mA, slit width 0.5 nm, working range 0.1−30 μg/mL). The pH of the adsorptive solution was adjusted by the addition of 0.01 N NaOH or 0.01 N HNO_3 as needed. The sets of conditions for the different experiments are given in Table 1.

The equations used for various computations are given in Table 2.[44−54]

3. Results and Discussion

3.1. Adsorbent Characterization. 3.1.1. XRD Study. Intercalation followed by calcination of a material usually results in reduction of crystallinity[55,56] and the material becomes amorphous to XRD. Calcination leads to a decrease in the basal spacings, which is sometimes accompanied by structural col-

Table 2. Models and Equations Used in This Work

parameters	theoretical model	equations	ref
isotherm	Freundlich	$q_e = K_f C_e^n$	44
	Langmuir	$C_e/q_e = 1/(bq_m) + (1/q_m)C_e$	45
	separation factor	$R_L = 1/(1 + bC_e)$	46
kinetics	first-order kinetics	$\ln(q_e - q_t) = \ln q_e - k_1 t$	47, 48
	second-order kinetics	$t/q_t = 1/(k_2 q_e^2) + (1/q_e)t$	49
	Elovich equation	$q_t = \beta \ln(\alpha\beta) + \beta \ln t$	50, 51
	intraparticle diffusion	$q_t = k_i t^{0.5}$	52
	liquid film diffusion	$\ln(1 - F) = - k_{fd} t$	53
thermodynamics		$\Delta G = - RT \ln K_d$	54
		$\Delta G = \Delta H - T\Delta S$	54
		$\ln K_d = \Delta S/R - \Delta H/RT$	54

lapse. The intercalated clays are usually better ordered than their parent clays, but this ordering cannot withstand calcination, which is reflected in fewer XRD peaks or no low-angle peaks.[55] The long-range ordering in the *c* direction either disappears or becomes less prominent after calcination. A considerable widening of the tip width was also noticed for the XRD peaks of the modified clays.

In accordance with the above observations, the intercalated clays show considerable loss of crystallinity after calcination accompanied by loss in number and intensity of the XRD peaks (Figure 1). The number of peaks in the range of 1−30° (2θ) decrease from seven (pure, calcined kaolinite) to five for ZrO−kaolinite and to one for TBA−kaolinite. A general widening of the XRD peaks and loss of intensity is also a common feature. The XRD peaks become less intense compared to those of the pure, calcined kaolinite [e.g., the 12.35° (2θ) peak has an intensity of only 73.4% for ZrO−kaolinite compared to the intensity of 99.6% for the pure, calcined kaolinite]. The intensity decrease is, however, much less for TBA−kaolinite.

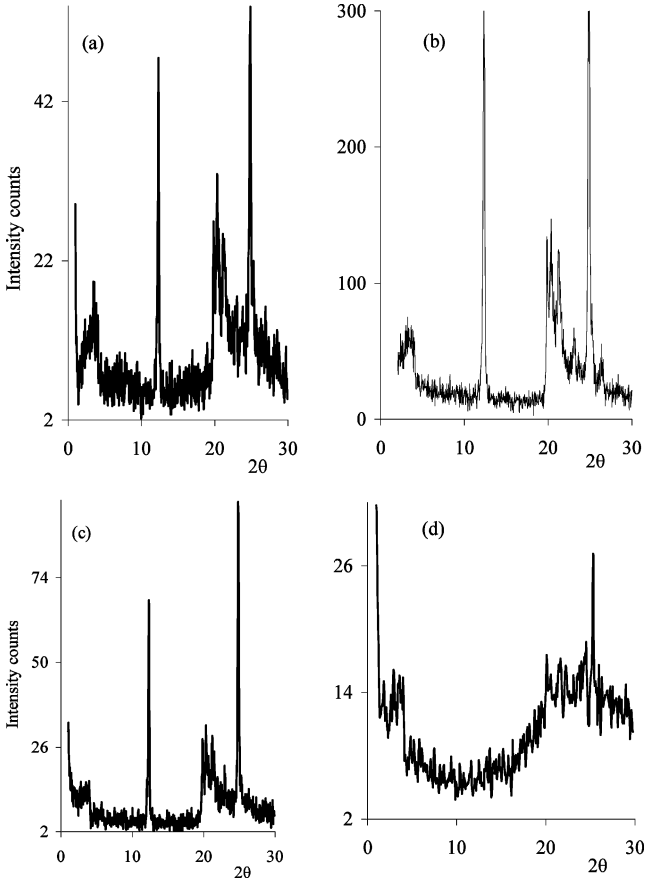

Figure 1. XRD patterns for (a) kaolinite (K1), (b) acid-activated kaolinite (K2), (c) ZrO−kaolinite (K3), and (d) TBA−kaolinite (K4).

When pure, calcined kaolinite is modified to ZrO−kaolinite, the tip width of the 12.35° (2θ) peak changes from 0.10 to 0.16. Similarly, the tip width of the 21.28° (2θ) peak changes from 0.16 to 0.24 when pure, calcined kaolinite is modified to TBA−kaolinite.

The XRD pattern of the acid-activated kaolinite shows lowering and widening of the characteristic peaks, implying a decrease in the regular pattern of the clay structure and a partial destruction of the structure compared to the parent clay.[25] The dispersion and amorphization of the acid-treated clay minerals are known to give rise to an increase in the intensities of the very low angle diffraction bands.[57] Similar results obtained in the present work are summarized below:

(i) For calcined, acid-activated kaolinite, the basal spacing expands from 4.452 to 4.462 Å (2θ = 19.92°), which is accompanied by a decrease in intensity from 23.14 to 21.32%.

(ii) The relative intensity of a low-angle peak occurring at 5.70° (2θ) increases from 1.28% (kaolinite) to 4.44% (acid-activated kaolinite).

3.1.2. Surface Area. The specific surface area of kaolinite (K1) is only 3.8 m^2/g, but it increase to 15.6 m^2/g for acid-activated kaolinite (K2), 13.4 m^2/g for the ZrO−kaolinite (K3), and 14.0 m^2/g for the TBA derivative (K4). The surface area of kaolinite is reported as 5−25 m^2/g.[58] Similar results have been reported by other authors.[55,56] Jobstmann and Singh[59] suggested that intercalation creates a porous framework, increasing the surface area of clay mineral. No report on the effect of acid treatment on the specific surface area of kaolinite could be found. However, the acid treatment opens up the edges of the platelets and, as a consequence, the surface area and the pore diameter increase,[60] which is in conformity with the results obtained in this work.

3.1.3. Cation Exchange Capacity (CEC). The CEC of kaolinite is measured as 11.3 mequiv/100 g, which is in agreement with the reported values.[61] Intercalation and calcination has a drastic effect on the CEC of the derivative clays, resulting in a decrease in the values. On acid treatment, the CEC of kaolinite increases to 12.2 mequiv/100 g. ZrO−kaolinite and TBA−kaolinite have CEC values of 10.2 and 3.9 mequiv/100 g, respectively. The large cations (ZrO^{2+} and TBA^+) may mask some of the exchangeable cations in the interlayer space, leading to a decrease in CEC. Similar results have been reported.[59]

The ion exchange capacity of clay minerals is attributed to structural defects, broken bonds, and structural hydroxyl transfers.[25] Acid treatment marginally increases the total number of exchange sites (CEC increase ~ 8%). The treatment of the clay with 0.25 M H_2SO_4 results in replacement of a number of different cations with H^+ ions, and on subsequent heating and calcination, dehydroxylation occurs, leaving behind a number of Lewis sites. Much of the increase in CEC in the present work is likely to be due to an increase in Lewis acidity as the acid-

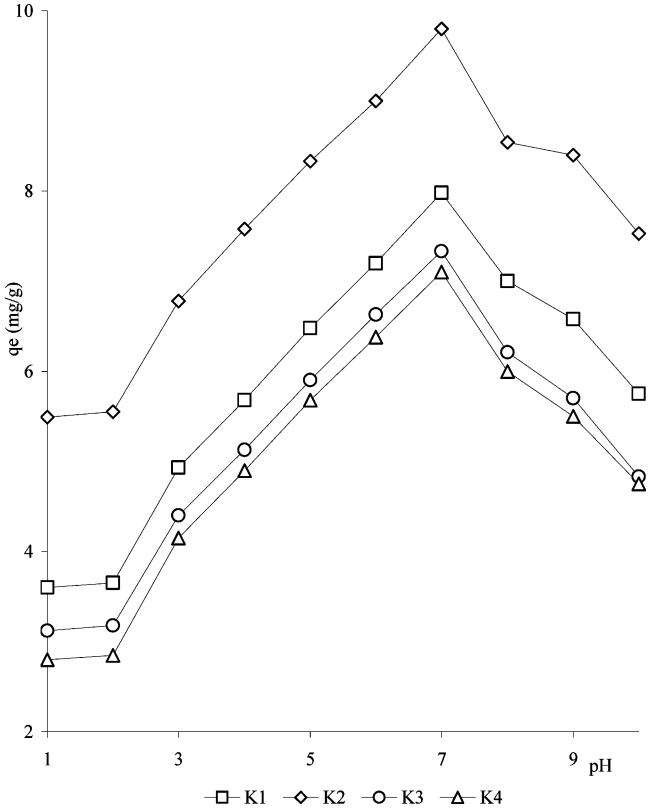

Figure 2. Influence of pH on adsorption of Cr(VI) on kaolinite (K1), acid-activated kaolinite (K2), ZrO−kaolinite (K3), and TBA−kaolinite (K4) at 303 K (clay 2 g/L, initial Cr(VI) 50 mg/L, time 240 min).

treated clay was calcined at 773 K before CEC measurement. The CEC increase may be a complex process involving these effects as well.

3.2. Adsorption of Cr(VI). 3.2.1. Effects of pH. The pH of the aqueous solution is a significant controlling factor in adsorption mechanism. The amount of Cr(VI) adsorbed per unit mass of clay increase up to pH 7.0, after which it shows a steady decrease (Figure 2). At a lower pH, the molecular form is the predominantly adsorbed species, while at a higher pH the ionized form is preferentially adsorbed.[62] For adsorption on bentonite surface, Khan et al.[63] have suggested that the Cr(VI) ions bind to OH groups in the anionic form as $HCrO_4^-$ at very low pH as the surface gets positively charged, while cationic adsorption takes place at increasing pH. On a variety of low-cost adsorbents such as wool, olive cake, sawdust, pine needles, almond, coal, and cactus leaves, Dakiky et al.[64] found maximum adsorption of Cr(VI) at pH 2.0 and suggested that the dominant adsorbed species was $HCrO_4^-$. Bayat[65] suggested a mechanism for adsorption of Cr(VI) at different pH values involving the species $HCrO_4^-$, H_2CrO_4, CrO_3, and $Cr_2O_7^{2-}$ as shown by

$$2H^+ + 2HCrO_4^- \overset{2H^+}{\leftrightarrow} 2H_2CrO_4 \leftrightarrow 2H_2O + Cr_2O_7^{2-} \overset{2H^+}{\leftrightarrow} 2CrO_3 + H_2O$$

The species H_2CrO_4 and CrO_3 have been proposed to exist as polynuclear species, along with their anhydrous forms, at high Cr(VI) concentration and at low pH. Some authors have proposed that, at low pH, the metal ions compete with H^+ ions for adsorption and, consequently, uptake of Cr(VI) decreased with lowering of pH.[16] While this may be true for most metal ions, the scenario is different with Cr(VI) as the predominant species is anionic. The decreased adsorption of Cr(VI) at low pH in the present work may be not due to competition with H^+ ions but due to competition with NO_3^- ions introduced inadvertently in the form of dilute nitric acid for attaining low pH.

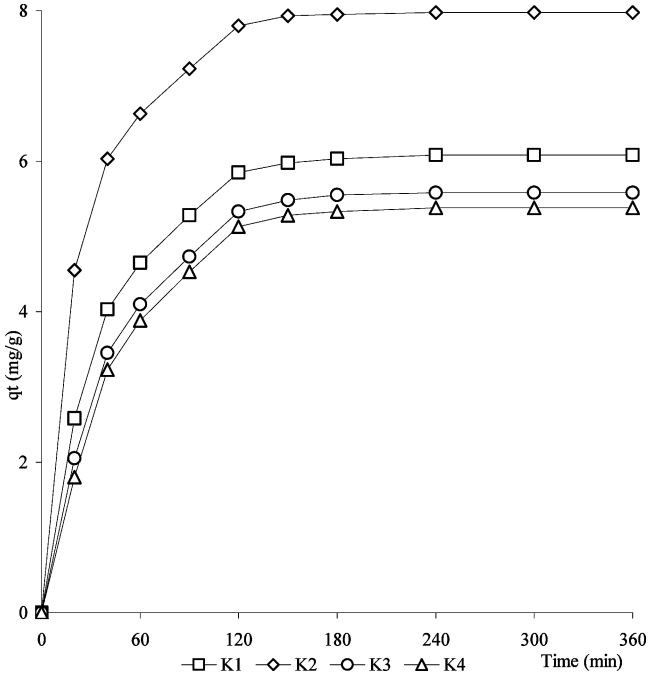

Figure 3. Effects of interaction time on adsorption of Cr(VI) on kaolinite (K1), acid-activated kaolinite (K2), ZrO−kaolinite (K3), and TBA−kaolinite (K4) at 303 K (clay 2 g/L, initial Cr(VI) 50 mg/L, pH 4.6).

Maximum adsorption of Cr(VI) on clay surface is observed at pH 7.0, after which adsorption again decreases. The formation of hydroxyl complexes of chromium, $Cr(OH)_3$, may be responsible for the decrease in adsorption which hinders the diffusion of Cr(VI) ions to the clay surface for undergoing adsorption. Similar results have been reported by Rengaraj et al.,[66] for the adsorption of Cr(VI) on ion exchange resins, where percent Cr(VI) adsorption showed a decreasing trend after pH 6.0.

At the same pH, adsorption of Cr(VI) experiences a jump when the acid-activated kaolinite (Figure 2) is the adsorbent. This shows that acid activation increases the number of adsorption sites for Cr(VI), resulting in a higher adsorption capacity compared to the nonactivated kaolinite at any pH. However, the introduction of Zr(hydr)oxide or TBA to kaolinite does not improve the adsorption capacity. The obvious reason is the blocking of the negatively charged sites and the pores by the poly(hydroxozirconium) ions or TBA ions. Similar results have been reported by Jobstmann and Singh[59] for adsorption of Cd(II) by hydroxyaluminum interlayered montmorillonite. The order of Cr(VI) uptake among the four clay adsorbents are acid-activated kaolinite (K2) > nonactivated kaolinite (K1) > ZrO−kaolinite (K3) > TBA−kaolinite (K4).

3.2.2. Effects of Interaction Time and Kinetics of Adsorption. Clay−Cr(VI) interaction is studied as a function of time, and the amount of Cr(VI) adsorbed per unit mass of clay adsorbents increases gradually with more and more metal ions in the adsorbate solution (Figure 3). The adsorption required about 240 min to reach near-equilibrium conditions. Daneshvar et al.[67] also reported similar results for Cr(VI) removal on soya cake with 300 min as the equilibrium time. Of all the clay adsorbents, acid-activated kaolinite showed the highest adsorption for Cr(VI).

At low coverage, Cr(VI) adsorption is very rapid, but as the coverage increases, the number of available surface sites come

Table 3. Rate Coefficients for Adsorption of Cr(VI) on Kaolinite (K1), Acid-Activated Kaolinite (K2), ZrO−Kaolinite (K3), and TBA−Kaolinite (K4) at 303 K[a]

parameters		K1	K2	K3	K4
pseudofirst order	$k_1 \times 10^2$ (min^{-1})	2.7	3.2	3.0	2.7
	r	−0.99	−0.99	−0.99	−0.99
pseudosecond order	$k_2 \times 10^2$ (g mg^{-1} min^{-1})	4.9	6.8	4.0	3.6
	r	+0.99	+0.99	+0.99	+0.99
Elovich model	$\alpha \times 10^3$ (g mg^{-1} min^2)	67.9	193.6	25.5	16.8
	β (mg g^{-1} min^{-1})	1.5	1.4	1.5	1.5
	r	+0.98	+0.97	+0.98	+0.98
intraparticle diffusion	$k_i \times 10$ (mg g^{-1} min$^{-0.5}$)	3.1	3.0	3.2	3.2
	intercept	2.0	4.0	1.4	1.1
	r	+0.92	+0.92	+0.93	+0.93
liquid film diffusion	$k_{fd} \times 10^2$ (min^{-1})	2.7	3.2	3.0	2.7
	intercept	−0.1	−0.1	−0.4	−0.3
	r	+0.99	+0.99	+0.98	+0.99

[a] Conditions: clay 2 g/L, initial Cr(VI) 50 mg/L, pH 4.6.

Table 4. Experimental and Computed q_e Values from Lagergren and Second-Order Plots for Adsorption of Cr(VI) on Kaolinite (K1), Acid-Activated Kaolinite (K2), ZrO−Kaolinite (K3), and TBA−Kaolinite (K4) at 303 K[a]

	q_e (mg/g)				
adsorbents	exptl	Lagergren	deviation (%)	second order	deviation (%)
K1	6.1	6.7	9.8	6.9	13.1
K2	8.0	8.1	1.3	8.7	8.8
K3	5.6	8.3	48.2	6.6	17.9
K4	5.4	7.1	31.5	6.5	20.4

[a] Conditions: clay 2 g/L, initial Cr(VI) 50 mg/L, pH 4.6.

down, and the rate decreases until equilibrium is approached. At equilibrium, the uptake is controlled by the rate at which the metal ions are transported from the external surface to the interior sites of adsorbents.[68] Different models are used to test the kinetics of Cr(VI)−clay interactions. The results are summarized in Table 3. The Lagergren log($q_e - q_t$) vs time plots are linear ($r = -0.99$) and the first-order rate constant varies between 2.7×10^{-2} and 3.2×10^{-2} min^{-1} for the four adsorbents (Table 3). The validity of the first-order kinetics is not good,[29] because the equilibrium adsorption capacity, q_e, obtained from the plots deviated by 1.3−48.2% (Table 4) from the experimental value at 240 min.

When second-order kinetics is applied, the t/q_t vs t plots are also linear ($r \sim +0.99$) and the second-order rate constant, k_2, varies from 3.6×10^{-2} to 6.8×10^{-2} g mg^{-1} min^{-1} (Table 3). Acid activation raises the second-order rate constant, indicating a faster interaction due to acid activation and a stronger affinity toward Cr(VI). The deviations in the q_e values (experimental and those obtained from the slopes of the second-order plots) are now in the range of 8.8−20.4%.

It should be noted that the deviations between theoretical and experimental q_e values (Table 4) are less for nonactivated kaolinite (K1) and acid-activated kaolinite (K2), with respect to both first-order and second-order kinetic models, but ZrO−kaolinite (K3) and TBA−kaolinite (K4) exhibit large variations in both cases.

For chemisorption on highly heterogeneous adsorbents, the Elovich equation sometimes gives a better account of the second-order kinetics. In the present work, the Elovich plots (q_t vs ln t) also have good linearity ($r \sim +0.97$ to $+0.98$) and the values of the coefficient α (1.68×10^{-2}−19.36×10^{-2} g mg^{-1}min^2) (Table 3) indicate rapid initial intake.[50] α for the acid-activated kaolinite (K2) is almost 3 times that for the nonactivated kaolinite (K1). This indicates formation of a comparatively larger number of chemisorptive bonds between acid-activated kaolinite and Cr(VI) ions than in the case of nonactivated kaolinite and Cr(VI). Both ZrO−kaolinite and TBA−kaolinite have lower α values than those of the nonactivated and acid-activated kaolinite, although between the two, the TBA derivative has a slightly higher value. The other coefficient, β, does not show much variation for all four adsorbents.

The plots (q_t vs $t^{0.5}$) for intraparticle diffusion similarly yield linear curves ($r \sim +0.92$ to $+0.93$) and the values of the rate constant, k_i, are given in Table 3. Significantly, the plots do not have a zero intercept (range 1.1−4.0), indicating that the diffusion of Cr(VI) species into the pores is not the dominating factor controlling the mechanism of the process. Similar results are obtained with the liquid film diffusion model involving diffusion from the bulk liquid phase to the surface of the adsorbent. The plots of $-\ln(1 - F)$ vs t are linear ($r \sim +0.98$ to 0.99) with intercepts of -0.1 to -0.4 (Table 3). The model requires the curves to pass through the origin, and although the intercepts are not zero, their small values signify some definite role for diffusion from the liquid phase to the adsorbent surface. The film diffusion rate coefficient is in the range 2.7×10^{-2}−3.2×10^{-2} min^{-1} (Table 3).

The uptake of Cr(VI) on the clays is thus not expected to follow simple kinetic models, and a number of mechanisms might be effective at the same time governing the adsorption processes.

3.2.3. Effects of adsorbent and adsorbate amount. When the amount of the adsorbent is increased from 2 to 6 g/L (Cr(VI) 50 mg/L), the adsorption also increases: from 24.3 to 39.4% for K1, from 31.9 to 46.3% for K2, from 22.2 to 36.6% for K3, and from 21.5 to 34.8% for K4. However, the increase is not enough to cause an increase in amount adsorbed per unit mass (q_e), which actually showed a decreasing trend (Figure 4). Similar results have been obtained by other workers.[66] This may be due to the following: (i) a large adsorbent amount reduces the unsaturation of the adsorption sites and, correspondingly, the number of such sites per unit mass comes down,

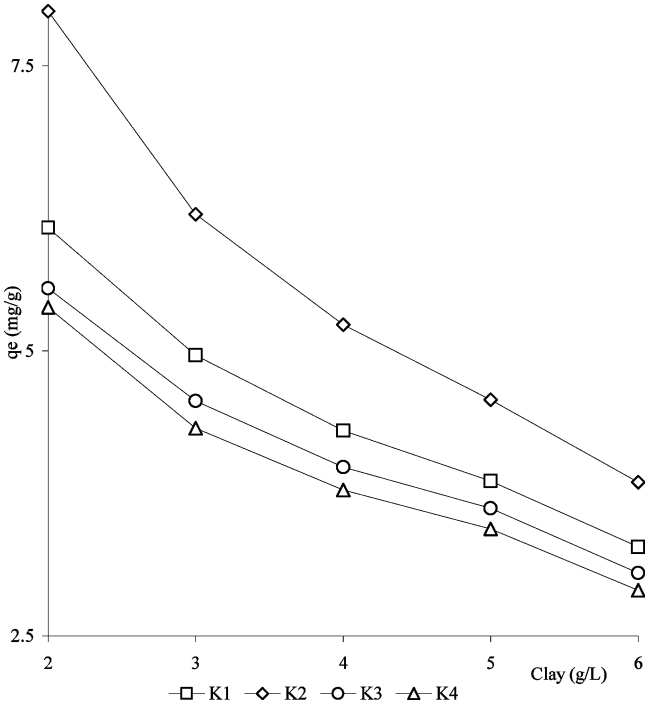

Figure 4. Influence of adsorbent amount on adsorption of Cr(VI) on kaolinite (K1), acid-activated kaolinite (K2), ZrO−kaolinite (K3), and TBA−kaolinite (K4) at 303 K (initial Cr(VI) 50 mg/L, pH 4.6, time 240 min).

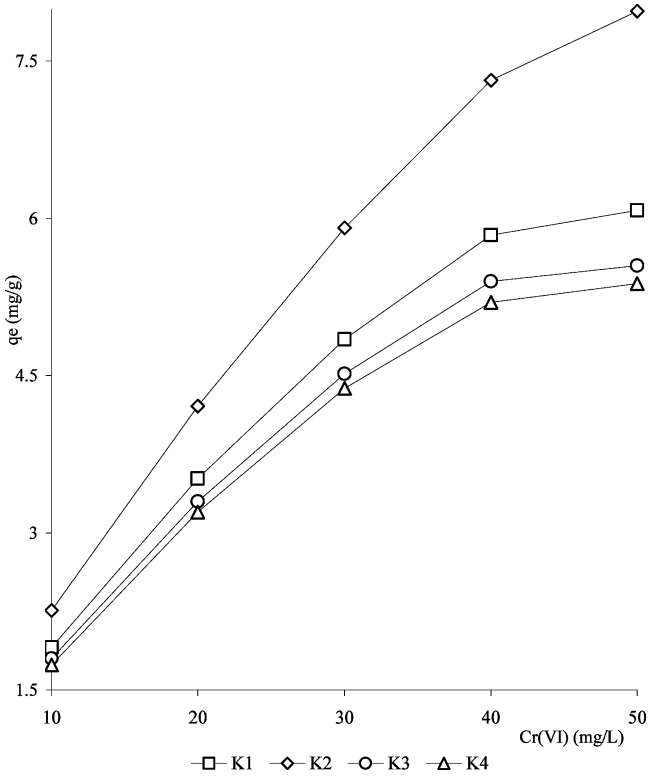

Figure 5. Effects of Cr(VI) concentration for adsorption on kaolinite (K1), acid-activated kaolinite (K2), ZrO−kaolinite (K3), and TBA−kaolinite (K4) at 303 K (clay 2 g/L, pH 4.6, time 240 min).

resulting in comparatively less adsorption at higher adsorbent amount; (ii) higher adsorbent amount creates particle aggregation, resulting in a decrease in the total surface area and an increase in diffusional path length, both of which contribute to a decrease in amount adsorbed per unit mass.[68]

When the initial concentration of Cr(VI) is varied from 10 to 50 mg/L at a constant clay amount of 2 g/L, the extent of adsorption (percent) decreases as expected from 38.1 to 24.3% for K1, from 45.2 to 31.9% for K2, from 35.9 to 22.2% for K3, and from 34.8 to 21.5% for K4. The amount adsorbed per unit mass, however, shows a gradual increase with more and more metal ions in the adsorbate solution (Figure 5). At low initial metal ion loading, the ratio of the number of Cr(VI) ions to the number of available adsorption sites on clays is small and consequently the adsorption is independent of the initial concentration. With an increase in the number of metal ions, the situation changes and the number of ions available per unit volume of the solution rises. This results in an increased competition for the binding sites[70] resulting in a decrease in percentage adsorption at high adsorbate loading. However, unit mass of the adsorbent is now exposed to a larger number of metal ions, resulting in a higher uptake by unit mass and consequently an increase in q_e. Similar results have been reported for the removal of Cr(VI) on maple sawdust by Yu et al.[16]

3.2.4. Adsorption isotherm. The empirical Freundlich isotherm yields good linear plots ($r \sim +0.95$ to $+0.97$). The values of the adsorption coefficients obtained from the plots are given in Table 5. The coefficients n and K_f have very similar values for the four adsorbents (n 0.4; K_f 0.9−1.5 $mg^{1-1/n}$ $L^{1/n}$ g^{-1}). The adsorption intensity $n < 1$ indicates favorable adsorption. The values of the adsorption capacity, K_f, are in the order K2 (acid-activated kaolinite) > K1 (nonactivated kaolinite) > K3 (ZrO−kaolinite) > K4 (TBA−kaolinite).

The Langmuir plots are also linear with $r \sim +0.99$ (Table 5). The values of the Langmuir equilibrium coefficient, b, are in a narrow range of 29.7−39.3 L g^{-1}, and these comparatively large values show that the equilibrium

$$\text{clay(solid phase)} + \text{Cr(VI)(aqueous phase)} = \text{clay}\cdots\text{Cr(VI)(adsorption complex)}$$

shifts to the right, i.e., toward the formation of the adsorbate−adsorbent complex. The Langmuir monolayer capacity, q_m, has values of 10.6 mg g^{-1} (TBA−kaolinite, K4) to 13.9 mg g^{-1} (acid-activated kaolinite, K2). Acid activation has a positive influence on the monolayer capacity of kaolinite mineral. The q_m values follow the same order as with the Freundlich adsorption capacity, i.e., K2 > K1 > K3 > K4. The separation factor $R_L \ll 1.0$ (values 0.0007−0.0010), indicating that the metal ions prefer to be in the bound state with the clay surface.

Dakiky et al.[64] have reported q_m values from 6.78 to 41.15 mg g^{-1} and K_f values from 0.094 to 2.23 L g^{-1} for adsorption of Cr(VI) on low-cost adsorbents such as wool, olive cake, sawdust, pine needles, almond, coal, and cactus at 303 K and pH 2.0. Babel and Kurniawan[71] studied Cr(VI) adsorption on coconut shell charcoal and commercial activated carbon modified with oxidizing agents and chitosan and reported q_m, b, R_L, and k_f values in the ranges of 2.18−10.88, 0.209−0.149, 0.161−0.217, and 0.61−1.84, respectively. These results may be comparable to those found in the present work.

3.2.5. Thermodynamic Studies. Appreciable variations in the Cr(VI) uptake are observed with the amount adsorbed per unit mass showing a rising trend with increase in temperature from 303 to 313 K. An increase in temperature helps more of the Cr(VI) ions to overcome the adsorption activation energy barrier and become attached to the clay surface.[72]

The thermodynamic parameters, ΔH, ΔS, and ΔG, for the adsorption process are computed from the plots of ln K_d vs $1/T$ (Table 6). Typical plots of ln K_d vs $1/T$ are given in Figure 6.

Table 5. Freundlich and Langmuir Coefficients for Adsorption of Cr(VI) on Kaolinite (K1), Acid-Activated Kaolinite (K2), ZrO−Kaolinite (K3), and TBA−Kaolinite (K4) at 303 K[a]

	Freundlich coefficients			Langmuir coefficients			
adsorbents	K_f ($mg^{1-1/n}$ $L^{1/n}$ g^{-1})	n	r	q_m (mg g^{-1})	b (L g^{-1})	r	R_L
K1	1.1	0.4	+0.96	11.6	32.2	+0.99	0.0008
K2	1.5	0.4	+0.95	13.9	39.3	+0.99	0.0007
K3	1.0	0.4	+0.96	10.9	31.0	+0.99	0.0009
K4	0.9	0.4	+0.97	10.6	29.7	+0.99	0.0010

[a] Conditions: clay 2 g/L, initial Cr(VI) 10, 20, 30, 40, 50, 75, 100, 150, 200, 250 mg/L, pH 4.6, time 240 min.

Table 6. Thermodynamic Data for Adsorption of Cr(VI) on Kaolinite (K1), Acid-Activated Kaolinite (K2), ZrO−Kaolinite (K3), and TBA−Kaolinite (K4)[a]

	adsorbents			
parameters	K1	K2	K3	K4
ΔH (kJ mol^{-1})	30.4	63.9	30.5	32.1
ΔS (J K^{-1} mol^{-1})	88.4	198.1	87.8	92.5
$-\Delta G$ (kJ mol^{-1})				
303 K	26.8	59.9	26.5	28.0
308 K	27.2	60.9	27.0	28.4
313 K	27.6	61.9	27.5	28.9

[a] Conditions: clay 2 g/L, pH 4.6, time 240 min.

The adsorption enthalpy, ΔH, is in the range of 30.4−63.9 kJ mol^{-1}, indicating that the overall adsorption process is endothermic. The values of ΔH are high enough to ensure strong interaction between the metal ions and the clay. Endothermic adsorption of Cr(VI) was observed by other authors.[63]

The values of the entropy change, ΔS, are in the range of 87.8−198.1 J K^{-1} mol^{-1}. Although the interactions are not expected to lead to any major change in surface configuration upon adsorption, a considerable entropy increase signifies an increased randomness at the solid−solution interface following the adsorption process.[73] Therefore, some structural changes and adjustments in both the adsorbate and adsorbent during the absorption process cannot be ruled out.[10] The adsorption interactions, being endothermic, are entropically driven. The increase in entropy probably arises from the release of ions such as H^+ and K^+ from the clay surface into the solution and also from partial desolvation of the metal ions.[35]

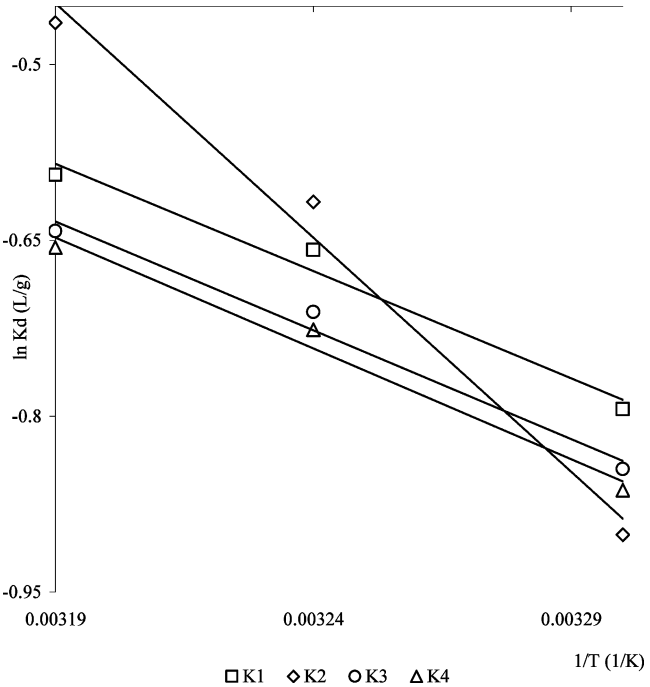

Figure 6. Plots of ln K_d vs $1/T$ for Cr(VI) adsorbed on kaolinite (K1), acid-activated kaolinite (K2), ZrO−kaolinite (K3), and TBA−kaolinite (K4) (clay 2 g/L, initial Cr(VI) 50 mg/L, pH 4.6, time 240 min).

Spontaneity of the adsorption process is established by a decrease in Gibbs energy, ΔG, from −26.8 to −27.6 kJ mol^{-1} (K1), from −59.9 to −61.9 kJ mol^{-1} (K2), from −26.5 to −27.5 kJ mol^{-1} (K3), and from −28.0 to − 28.9 kJ mol^{-1} (K4) in the temperature range of 303−313 K. The large decrease in Gibbs energy shows that the Cr(VI)−clay adsorption complex is much more stable and is held very strongly to the clay surface, which is favored by an increase in temperature. The decrease in Gibbs energy was the largest for K2, reflecting a much more energetically favorable process[64] for adsorption of Cr(VI) on this acid-activated clay.

The thermodynamic data on metal adsorption on clays are limited. Yuvaz et al.[34] have found that ΔH, ΔS, and ΔG for adsorption of Cu(II) on Turkish kaolinite are 39.52 kJ mol^{-1}, 11.7 J K^{-1} mol^{-1}, and 4.61 kJ mol^{-1}, respectively. The ΔH values are very close to the ones obtained in the present work (except K2), but higher ΔS values indicate that Cr(VI)−clay interactions are much more entropically driven than in the case of Cu(II)−kaolinite interaction. Moreover, Cr(VI)−clay interactions are accompanied by a larger decrease in Gibbs energy than in the case of Cu(II)−kaolinite interactions.

4. Conclusions

Clay minerals (kaolinite, acid-activated kaolinite, poly(oxozirconium) kaolinite, and tetrabutylammonium kaolinite) are capable of removing Cr(VI) from an aqueous solution. Treatment of kaolinite with acid improved its adsorption capacity, but introduction of poly(oxozirconium) and tetrabutylammonium ions into kaolinite did not increase the capacity of kaolinite to take up more Cr(VI) ions. The surface area of kaolinite increases on acid activation as well as by introduction of either ZrO or TBA, but the cation exchange capacities (CECs) of the ZrO and TBA derivatives decrease relative to the original untreated kaolinite. The acid activation, however, has a positive influence on the CEC, and it is found that the CECs are in the order of acid-activated kaolinite (K2) > kaolinite (K1) > ZrO−kaolinite (K3) > TBA−kaolinite (K4). The introduction of ZrO or TBA into kaolinite has resulted in a product of smaller CEC and larger external specific surface. This may be responsible for lowering the adsorption capacities of ZrO−kaolinite and TBA−kaolinite compared to the untreated clay. The Cr(VI) adsorption capacity follows the same order as K2 > K1 > K3 > K4. Thus, though the untreated kaolinite has the smallest surface area of the four adsorbents, its capacity for Cr(VI) adsorption is higher than those of ZrO and TBA derivatives but lower than that of the acid-treated kaolinite.

The adsorption of Cr(VI) on clays reaches equilibrium around 240 min and intraparticle diffusion may not be very significant, while diffusion from the liquid film surrounding the clay particles into the surface may have a dominant role. The kinetics of clay−Cr(VI) interactions is very complex, and different models show that nonactivated kaolinite and acid-activated

kaolinite are likely to follow either a first-order or second-order mechanism, while the interactions of Cr(VI) with ZrO−kaolinite and TBA−kaolinite are more complicated.

The adsorption data agree well with Langmuir and Freundlich isotherms, and the adsorption coefficients support the conditions of favorable adsorption. Thermodynamically, the interactions are endothermic, are entropically driven, and are supported by a decrease in Gibbs energy.

The kaolinite adsorbents loaded with Cr(VI) do not desorb the toxic metal easily simply on vigorous agitation. However, more work needs to be done on desorption aspects and subsequently on recovery of Cr(VI) and disposal of the loaded adsorbents.

Acknowledgment

S.S.G. is grateful to the University Grants Commission for providing assistance under the Faculty Improvement Programme. The authors are grateful to the three reviewers for very useful comments and for pointing out various errors and omissions.

Nomenclature

C_o = initial concentration of the Cr(VI), mg/L
C_e = equilibrium concentration of Cr(VI) in liquid phase, mg/L
q_e = equilibrium concentration of Cr(VI) in solid phase (i.e., amount of Cr(VI) adsorbed per unit mass at equilibrium), mg/g
q_t = amount of Cr(VI) adsorbed per unit mass at any time t, mg/g
K_f = Freundlich coefficient for adsorption capacity, $mg^{1-1/n}\ L^{1/n}\ g^{-1}$
n = Freundlich coefficient for adsorption intensity
b = Langmuir coefficient for adsorbate−adsorbent equilibrium, $L\ g^{-1}$
q_m = Langmuir monolayer adsorption capacity, $mg\ g^{-1}$
R_L = dimensionless separation factor
k_1 = pseudo-first-order adsorption rate constant, min^{-1}
k_2 = second-order rate constant, $g\ mg^{-1}\ min^{-1}$
α = Elovich coefficient for initial adsorption rate, $g\ mg^{-1}\ min^2$
β = Elovich coefficient for desorption coefficient, $mg\ g^{-1}\ min^{-1}$
k_i = intraparticle diffusion rate constant, $mg\ g^{-1}\ min^{-0.5}$
F = fractional attainment of equilibrium ($=q_t/q_e$)
k_{fd} = film diffusion rate constant, min^{-1}
ΔH = enthalpy of adsorption, $kJ\ mol^{-1}$
ΔS = entropy of adsorption, $J\ K^{-1}\ mol^{-1}$
ΔG = Gibbs free energy, $kJ\ mol^{-1}$
K_d = distribution coefficient of the adsorbate, $L\ g^{-1}$
T = temperature, K
R = gas constant, $kJ\ K^{-1}\ mol^{-1}$
r = regression coefficient
CEC = cation exchange capacity, mequiv/100 g
K1 = kaolinite
K2 = acid-activated kaolinite
K3 = ZrO−kaolinite
K4 = TBA−kaolinite

Literature Cited

(1) Chakir, A.; Bessiere, J.; Kacemi, K. EL.; Marouf, B. A comparative study of the removal of trivalent chromium from aqueous solutions by bentonite and expanded perlite. *J. Hazard. Mater.* **2002**, *95*, 29.

(2) Hayes, R. B. Review of occupational epidemiology of chromium chemicals and respiratory cancer. *Sci. Total Environ.* **1988**, *71*, 331.

(3) ATSDR. *Case Studies in Environmental Medicine: Chromium toxicity*; Agency for Toxic Substances and Disease Registry, US Department of Health and Human Services, Division of Health Education and Promotion: Atlanta, GA, 2000.

(4) Gupta, V. K.; Jain, C. K.; Ali, I.; Sharma, M.; Saini, V. K. Removal of cadmium and nickel from wastewater using bagasse fly ash—a sugar industry waste. *Water Res.* **2003**, *37*, 4038.

(5) Mathialagan, T.; Viraraghavan, T. Adsorption of cadmium from aqueous solutions by perlite. *J. Hazard. Mater.* **2002**, *94*, 291.

(6) Gupta, V. K.; Gupta, M.; Sharma, S. Process development for the removal of lead and chromium from aqueous solutions using red mud—an aluminium industry waste. *Water Res.* **2001**, *35*, 1125.

(7) Kadirvelu, K.; Namasivayam, C. Activated carbon from coconut coirpith as metal adsorbent: adsorption of Cd(II) from aqueous solution. *Adv. Environ. Res.* **2003**, *7*, 471.

(8) Pan, S. C.; Lin, C. C.; Tseng, D. H. Reusing sewage sludge ash as adsorbent for copper removal from wastewater. *Resour., Conserv. Recycl.* **2003**, *39*, 79.

(9) Chiron, N.; Guilet, R.; Deydier, E. Adsorption of Cu(II) and Pb(II) onto a grafted silica: isotherms and kinetic models. *Water Res.* **2003**, *37*, 3079.

(10) Ho, Y. S. Removal of copper ions from aqueous solution by tree fern. *Water Res.* **2003**, *37*, 2323.

(11) Ko, D. C. K.; Cheung, C. W.; Choy, K. K. H.; Porter, J. F.; McKay, G. Sorption equilibria of metal ions on bone char. *Chemosphere* **2004**, *54*, 273.

(12) Maity, S.; Chakravarty, S.; Bhattacharjee, S.; Roy, B. C. A study on arsenic adsorption on polymetallic sea nodule in aqueous medium. *Water Res.* **2005**, *39*, 2579.

(13) Wingenfelder, U.; Nowack, B.; Furrer, G.; Schulin, R. Adsorption of Pb and Cd by amine-modified zeolite. *Water Res.* **2005**, *39*, 3287.

(14) Srivastava, S. K.; Gupta, V. K.; Mohan, D. Kinetic parameters for the removal of lead and chromium from wastewater using activated carbon developed from fertilizer waste material. *Environ. Modell. Assess.* **1996**, *1*, 281.

(15) Gupta, V. K.; Srivastava, A. K.; Jain, N. Biosorption of chromium-(VI) from aqeous solutions by green algae Spirogyra species. *Water Res.* **2001**, *35*, 4079.

(16) Yu, L. J.; Shukla, S. S.; Dorris, K. L., Shukla, A.; Margrave, J. L. Adsorption of chromium from aqueous solutions by maple sawdust. *J. Hazard. Mater.* **2003**, *B100*, 53.

(17) Bayat, B. Comparative study of adsorption properties of Turkish fly ashes. II. The case of chromium(VI) and cadmium(II). *J. Hazard. Mater.* **2002**, *95*, 275.

(18) Gupta, V. K.; Ali, I. Removal of lead and chromium from wastewater using bagasse fly ash—a sugar industry waste. *J. Colloid Interface Sci.* **2004**, *271*, 321.

(19) Wang, S. L.; Hseu, R. J.; Chang, R. R.; Chiang, P. N.; Chen, J. H.; Tzou, Y. M. Adsorption and thermal desorption of Cr(VI) on Li/Al layered double hydroxide. *Colloids Surf., A: Physicochem. Eng. Aspects* **2006**, *277*, 8.

(20) Deer, W. A.; Howie, R. A.; Zussman, J. *An introduction to the rock-forming minerals*; ELBS Longman: Essex, England, 1985.

(21) Li, Z.; Bowman, R. S. Retention of inorganic oxyanions by organo-kaolinite. *Water Res.* **2001**, *35*, 3771.

(22) Jackson, M. L.; Sherman, G. D. Chemical weathering of clay minerals in soils. *Adv. Agron.* **1952**, *5*, 219.

(23) Eberl, D. D.; Velde, B.; McCormick, T. Synthesis of illite-smectite from smectite at earth surface temperatures and high pH. *Clay Miner.* **1993**, *28*, 49.

(24) Theocharis, C. R.; Jacob, K. J.; Gray, A. C. Enhancement of Lewis acidity in layer aluminosilicates. *J. Chem. Soc., Faraday Trans.* **1988**, *84*, 1509.

(25) Rodrigues, M. G. F. Physical and catalytic characterization of smectites from Boa-Vista, Paraiba, Brazil. *Ceramica* **2003**, *49*, 146.

(26) Burch, R.; Warburton, C. I. Zr containing pillared interlayered clays: 1. Preparation and structural characterization. *J. Catal.* **1986**, *97*, 503.

(27) Pereira, P. R.; Pires, J.; de Carvalho, M. B. Zirconium pillared clays for carbon dioxide/methane separation, 1. Preparation of adsorbent materials and pure gas adsorption. *Langmuir* **1998**, *14*, 4584.

(28) Lawrence, M. A. M.; Kukkadapu, R. K.; Boyd, S. A. Adsorption of phenol and Chlorinated phenols from aqueous solution by tetramethyl-ammonium- and tetramethylphosphonium-exchanged montmorillonite. *Appl. Clay Sci.* **1998**, *13*, 13.

(29) Stevens. J. J.; Anderson, S. J. An FTIR study of water sorption on TMA- and TMPA-montmorillonite. *Clays Clay Miner.* **1996**, *44*, 142.

(30) Ohtsuka, K.; Hayashi, Y.; Suda, M. Microporous ZrO2 pillared clays derived from three kinds of Zr polynuclear ionic species. *Chem. Mater.* **1993**, *5*, 1823.

(31) Echeverria, J. C.; Churio, E.; Garrido, J. Retention mechanisms of Cd on illite. *Clays Clay Miner.* **2002**, *50*, 614.

(32) Alvarez-Ayuso, E.; Garcia-Sanchez, A. Removal of heavy metals from wastewaters by natural and Na-exchanged bentonites. *Clays Clay Miner.* **2003**, *51*, 475.

(33) Kara, M.; Yuzer, H.; Sabah, E.; Celik, M. S. Adsorption of cobalt from aqueous solutions onto sepiolite. *Water Res.* **2003**, *37*, 224.

(34) Yavuz, O.; Altunkaynak, Y.; Guzel, F. Removal of copper, cobalt and manganese from aqueous solution by kaolinite. *Water Res.* **2003**, *37*, 948.

(35) Angove, M. J.; Johnson, B. B.; Wells, J. D. The influence of temperature on the adsorption of cadmium(II) and cobalt(II) on kaolinite. *J. Colloid Interface Sci.* **1998**, *204*, 93.

(36) Strawn, D. G.; Palmer, N. E.; Furnare, L. J.; Goodell, C.; Amonette, J. E.; Kukkadapu, R. K. Copper sorption mechanisms on smectites. *Clays Clay Miner.* **2004**, *52*, 321.

(37) Lin, S.-H.; Juang, R.-S. Heavy metal removal from water by sorption using surfactant-modified montmorillonite. *J. Hazard. Mater.* **2002**, *B92*, 315.

(38) De Leon, A. T.; Nunes, D. G.; Rubio, J. Adsorption of Cu ions onto a 1:10 phenanthroline-grafted Brazilian bentonite. *Clays Clay Miner.* **2003**, *51*, 58.

(39) Bhattacharyya K. G.; Sen Gupta, S. Pb(II) uptake by kaolinite and montmorillonite in aqueous medium: Influence of acid activation of the clays. *Colloids Surf., A: Physicochem. Eng. Aspects* **2006**, *277*, 191.

(40) Espantaleon, A. G.; Nieto, J. A.; Fernandez, M.; Marsal, A. Use of activated clays in the removal of dyes and surfactants from tannery waste waters. *Appl. Clay Sci.* **2003**, *24*, 105.

(41) Mortland, M. M.; Shaobai, S.; Boyd, S. A. Clay-organic complexes as adsorbents for phenol and chlorophenols. *Clays Clay Miner.* **1986**, *34*, 581.

(42) Sears, G. Determination of specific surface area of colloidal silica by titration with sodium hydroxide. *Anal. Chem.* **1956**, *28*, 1981.

(43) Bergaya, F.; Vayer, M. CEC of clays: Measurement by adsorption of a copper ethylendiamine complex. *Appl. Clay Sci.* **1997**, *12*, 275.

(44) Freundlich, H. M. F. Over the adsorption in solution. *J. Phys. Chem.* **1906**, *57*, 385.

(45) Langmuir, I. The adsorption of gases on plane surfaces of glass, mica and platinum. *J. Am. Chem. Soc.* **1918**, *40*, 1361.

(46) Hall, K. R.; Eagleton, L. C.; Acrivos, A.; Vermeulen, T. Pore- and solid-diffuion kinetics in fixed-bed adsorption under constant-pattern conditions. *Ind. Eng. Chem. Fundam.* **1966**, *5*, 212.

(47) Lagergren, S. Zur theorie der sogenannten adsorption gelöster stoffe. *Kungliga Svenska Vetenskapsakademiens. Handlingar* **1898**, 24 (4), 1.

(48) Ho, Y. S. Citation review of Lagergren kinetic rate equation on adsorption reactions. *Scientometrics* **2004**, *59*, 171.

(49) Ho, Y. S.; Ng, J. C. Y.; McKay, G. Removal of lead(II) from effluents by sorption on peat using second-order kinetics. *Sep. Sci. Technol.* **2001**, *36*, 241.

(50) Ho, Y. S.; McKay, G. Application of kinetic models to the sorption of copper(II) on to Peat. *Adsorpt. Sci. Technol.* **2002**, *20*, 797.

(51) Chien, S.; Clayton, W. R. Application of Elovich equation to the kinetics of phosphate release and sorption in soils. *Soil Sci. Soc. Am. J.* **1980**, *44*, 265.

(52) Weber, W. J.; Morris, J. C. Kinetics of adsorption of carbon from solutions. J. *Sanit. Eng. Div. Am. Soc. Civ. Eng.* **1963**, *89*, 31.

(53) Boyd, G. E.; Adamson, A. W.; Myers, L. S. The exchange adsorption of ions from aqueous solutions on organic zeolites. Kinetics II. *J. Am. Chem. Soc.* **1947**, *69*, 2836.

(54) Thomas, W. J.; Crittenden, B. *Adsorption Technology and Design*; Butterworth-Heinemann: Oxford, 1998.

(55) Grzybek, T.; Klinik, J.; Olszewska, D.; Papp, H.; Smarzowski, J. The Influence of montmorillonite treatment on structure, sorption properties and catalytic behaviour: Part I. Zirconia pillared clays modified with manganese as denox catalyts. *Pol. J. Chem.* **2001**, *75*, 857.

(56) Valverde, J. L.; Sanchez, P.; Dorado, F.; Asencio, I.; Romero, A. Preparation and characterization of Ti-pillared clays using Ti alkoxide. Influence of the synthesis parameters. *Clays Clay Miner.* **2003**, *51*, 41.

(57) Jozefaciuk, G.; Bowanko, G. Effect of acid and alkali treatments on surface areas and adsorption energies of selected minerals. *Clays Clay Miner.* **2002**, *50*, 771.

(58) Volzone, C.; Thompson, J. G.; Melnitchenko, A.; Ortiga, J.; Palethorpe, S. R. Selective gas adsorption by amorphous clay-mineral derivatives. *Clays Clay Miner.* **1999**, *5*, 647.

(59) Jobstmann, H.; Singh, B. Cadmium sorption by hydroxy-aluminium interlayered montmorillonite. *Water Air Soil Pollut.* **2001**, *131*, 203.

(60) Diaz, F. R. V.; Santos, P. D. S. Studies on the acid activation of Brazilian smectitic clays. *Quim. Nova* **2001**, *24*, 345.

(61) Grim, R. E. *Clay Mineralogy*; McGraw-Hill: New York, 1968.

(62) Sharma, A.; Bhattacharyya, K. G. Adsorption of Chromium(VI) on Azadirachta indica (Neem) leaf powder. *Adsorption* **2004**, *10*, 327.

(63) Khan, S. A.; Rehman, R.; Khan, M. A. Adsorption of chromium-(III), chromium(VI) and silver(I) on bentonite. *Waste Manage.* **1995**, *15*, 271.

(64) Dakiky, M.; Khamis, M.; Manassra, A.; Mer'eb, M. Selective adsorption of chromium(VI) in industrial wastewater using low-cost abundantly available adsorbents. *Adv. Environ. Res.* **2002**, *6*, 533.

(65) Bayat, B., Comparative study of adsorption properties of Turkish fly ashes. II. The case of chromium(VI) and cadmium(II). *J. Hazard. Mater.* **2002**, *95*, 275−290.

(66) Rengaraj, S.; Joo, C. K.; Kim, Y.; Yi, J. Kinetics of removal of chromium from water and electronic process wastewater by ion exchange resins: 1200H, 1500H and IRN97H. *J. Hazard. Mater.* **2003**, *B102*, 257.

(67) Daneshvar, N.; Salari, D.; Aber, S. Chromium adsorption and Cr-(VI) reduction to trivalent chromium in aqueous solutions by soya cake. *J. Hazard. Mater.* **2002**, *B94*, 49.

(68) Yu, B.; Zhang, Y.; Shukla, A.; Shukla, S. S.; Dorris, K. L. The removal of heavy metal from aqueous solutions by sawdust adsorption—removal of copper. *J. Hazard. Mater.* **2000**, *B80*, 33.

(69) Ho, Y. S.; McKay, G. Competitive sorption of copper and nickel ions from aqueous solution using peat. *Adsorption* **1999**, *5*, 409.

(70) Ucun, H.; Bayhan, Y. K.; Kaya, Y.; Cakici, A.; Algur, O. F. Biosorption of lead (II) from aqueous solution by cone biomass of Pinus sylvestris. *Desalination* **2003**, *154*, 233.

(71) Babel, S.; Kurniawan, T. A. Cr(VI) removal from synthetic wastewater using coconut shell charcoal and commercial activated carbon modified with oxidizing agents and/or chitosan. *Chemosphere* **2004**, *54*, 951.

(72) Shukla, A.; Zhang, Y.-H.; Dubey, P.; Margrave, J. L.; Shukla, S. S. The role of sawdust in the removal of unwanted materials from water. *J. Hazard. Mater.* **2002**, *35*, 137.

(73) Jain, C. K.; Sharma, M. K. Adsorption of cadmium on bed sediments of river Hindon: adsorption models and kinetics. *Water Air Soil Pollut.* **2002**, *137*, 1.

Received for review May 12, 2006
Revised manuscript received July 29, 2006
Accepted August 10, 2006

IE060586J